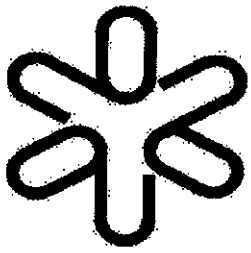

Instituto de Física
Universidade de São Paulo

THEORY OF MULTIPLE GIANT DIPOLE RESONANCE EXCITATION

CARLSON, B. V.; HUSSEIN, M. S.; TOLEDO PIZA, A. F. R.; CANTO, L. F.
DEPTO. FÍSICA NUCLEAR

Publicação IF - 1327/98

DEPARTAMENTO DE FÍSICA NUCLEAR
INSTITUTO DE FÍSICA
UNIVERSIDADE DE SÃO PAULO

IFUSP - DFN/98-003

Theory of Multiple Giant Dipole Resonance Excitation

B.V. Carlson
M.S. Hussein
A.F.R. de Toledo Piza
L.F. Canto

Theory of multiple giant dipole resonance excitation

B.V. Carlson

Departamento de Física,Instituto Tecnológico de Aeronáutica - CTA,

12228-900 São José dos Campos, SP, Brazil

M.S. Hussein and A.F.R. de Toledo Piza

Instituto de Física, Universidade de São Paulo,

C.P. 66318, São Paulo, 05315-970, Brazil

L.F. Canto

Instituto de Física, Universidade do Rio de Janeiro, CP 68528,

21945-970 Rio de Janeiro RJ, Brazil

Abstract

A semiclassical description of multiple giant resonance excitation that incorporates incoherent fluctuation contributions of the Brink-Axel type is developed. Numerical calculations show that the incoherent contributions are important at low to intermediate bombarding energies.

PACS Numbers: 25.70.De, 24.30.Cz, 21.10.Re

I. INTRODUCTION

The Coulomb excitation of two-phonon giant resonances at intermediate energies has generated considerable interest in the last few years [1]. The isovector double giant dipole resonance (DGDR) has been observed in ^{136}Xe [2], ^{197}Au [3], and ^{208}Pb [4–6]. The isoscalar double giant quadrupole resonance has also been observed in the proton emission spectrum from the collision of ^{40}Ca with ^{40}Ca at a laboratory energy of 44 A Mev [7]. When the

data on DGDR excitation for ^{136}Xe and ^{197}Au are compared with coupled-channel Coulomb excitation calculations [8], it is found that, in the harmonic approximation, the calculated cross sections are a factor of 2 to 3 smaller than the measured ones. A similar discrepancy, albeit somewhat smaller, is found for ^{208}Pb.

Several effects that are not taken into account in the coupled-channel theory have been considered as possible explanations of this discrepancy. As examples, we mention the effect of anharmonicities [9,10] and the quenching of the 1^+ DGDR state [11]. Here we will consider a potentially important mechanism, which consists in the Coulomb excitation of a GDR on the background states populated by the decay of a previously excited GDR [12–14], as shown in Fig. 1. The importance of such 'hot' collective excitations in nuclear gamma emission was suggested long ago by Brink and Axel [15]. Due to the complicated nature of the noncollective background states, the amplitude for this excitation process varies rapidly with energy and possesses an average close to zero. Its contribution to the cross section can be sizable, however.

The excitation of a second GDR after the decay of a first will be possible only if the decay occurs before the collision has ended. We can thus obtain an estimate of the relevance of this excitation mechanism by comparing the Coulomb collision time to the giant dipole resonance decay time. The decay time can be estimated as $\tau_d = \hbar/\Gamma_d$, where Γ_d is the giant resonance spreading width. For ^{208}Pb, the GDR width is $\Gamma_d \approx 4$ MeV, which yields $\tau_d \approx 16 \times 10^{-23}$ s. We estimate the collision time using the schematic time dependence of the Coulomb interaction of Ref. 8,

$$V(t) = \frac{V_0}{1 + (\gamma v t/b)^2}, \tag{1}$$

which furnishes a collision time of the order of $\tau_c \approx 2b/\gamma v$.

In Fig. 2, we compare the decay and collision times for the case of ^{208}Pb + ^{208}Pb, as a function of the incident energy per nucleon, using a value of 15 fm for the impact parameter b. We see that below about 150 MeV per nucleon, the collision time is longer than the decay time. We expect that the excitation of a second GDR after the decay of a first will be an

important process in this energy range, when compared to direct double GDR excitation. As the collision times decreases slowly with the incident energy, we expect it to remain important over an even wider energy range.

II. THE BRINK-AXEL MECHANISM AND THE EVOLUTION EQUATION

Giant resonances have many characteristics that suggest a treatment in terms of simple collective degrees of freedom. The first and foremost of these is their classical interpretation in terms of macroscopic shape oscillations of the nucleus. The properties of multiple excitations of these resonances would then suggest that they are simple bosonic degrees of freedom. The Brink-Axel hypothesis, which assumes that a giant dipole resonance may be constructed on each of the intrinsic excited states of the nucleus, suggests that the resonances can be considered as degrees of freedom independent of the intrinsic states. Of course, the microscopic representation of the giant resonances, in terms of of the intrinsic particle-hole states, implies that their treatment as independent degrees of freedom can only be approximate. Yet, in many instances, it seems to be a very good approximation.

We will treat the giant resonance as an independent degree of freedom and label the states of the nucleus with both a collective index n, denoting the number of collective dipole phonons, and a statistical one s, denoting the number of collective phonons that have decayed into the incoherent background. The class of states denoted by the pair of indices n and s thus possesses n phonons of collective excitation and an incoherent background excitation obtained through the decay of another s phonons. We will represent this class of states by a single state. In the limit of harmonic phonons, this state would have an excitation energy of $(n+s)\varepsilon_d$ and a width of $n\Gamma_d$, where ε_d is the energy of the giant dipole resonance and Γ_d is its spreading width. We neglect contributions of the escape widths, as these are extremely small when compared to those of the spreading widths of the systems of interest here [14]. A schematic representation of the states and the transitions between them is given in Fig. 3.

We will consider the Coulomb excitation of a collective degree of freedom of a projectile

nucleus by an inert target and the subsequent decay of the collective states into complex intrinsic ones. Although the collective excitation of the nucleus is a coherent process, its statistical decay is an incoherent one. The time evolution of the system thus possesses both coherent and incoherent aspects, making a density matrix formulation necessary. We consider the time evolution of the density matrix elements $\rho_{ns,n's'}(t)$. The diagonal element $\rho_{ns,ns}(t)$ represents the instantaneous occupation probability of the state with n collective phonons and a statistical background equivalent to s phonons.

Following Ref. 16, we can put the time-evolution equation of the semiclassical density matrix into the form

$$\begin{aligned}\hbar\frac{\partial\rho_{ns,n's'}}{\partial t} = &-i\sum_m\left\{\left(\varepsilon_n+\varepsilon_s\right)\delta_{nm}+V_{nm}(t)\right\}\rho_{ms,n's'}\\ &+i\sum_m\rho_{ns,ms'}\left\{\left(\varepsilon_{n'}+\varepsilon_{s'}\right)\delta_{mn'}+V_{mn'}(t)\right\}\\ &-\frac{\left(\Gamma_{ns}+\Gamma_{n's'}\right)}{2}\rho_{nsn's'}+\delta_{nn'}\delta_{ss'}\sum_{m,r}\Gamma_{ns\leftarrow mr}\rho_{mr,mr},\end{aligned} \tag{2}$$

The terms in the first two lines on the right-hand side induce the coherent contribution to the evolution. This is given in terms of the (diagonal) collective and statistical contributions to the excitation energy, ε_n and ε_s, and of the interaction V, which couples the states through collective excitation alone. The two terms on the third line describe, respectively, the loss of probability due to incoherent, statistical transitions out of the state and the gain of probability due to statistical transitions from the other states. The partial gain widths $\Gamma_{ns\leftarrow mr}$ are such that

$$\sum_{n,s}\Gamma_{ns\leftarrow mr}=\Gamma_{mr}. \tag{3}$$

This condition simply states that the sum of the partial widths for probability transfer from any one state to all others must be equal to the total width for probability loss from the initial state. This guarantees probability conservation during the evolution of the system (assuming, of course, that ε_n and ε_s are real and that $V(t)$ is Hermitian).

We note that the standard calculation of giant resonance excitation [8] assumes it to be a coherent process, with a wave function that evolves according to

$$\hbar\frac{\partial\psi_{n0}}{\partial t} = -i\sum_m \{\varepsilon_n\delta_{nm} + V_{nm}(t)\}\,\psi_{m0} - \frac{\Gamma_{n0}}{2}\psi_{n0}. \tag{4}$$

This expression takes into account the coherent excitation and subsequent decay of the GDR in the same manner as Eq. (2). However, due to its coherence, it cannot account for the probability that has decayed and thus lacks a gain term. The density matrix formalism of Eq. (2) and the additional statistical states are necessary to obtain a complete description of the time evolution.

We will assume that the initial population is in the ground state. The initial conditions for which the equation will be solved are then

$$\rho_{ns,n's'}(t \to -\infty) \to \delta_{nn'}\delta_{n0}\delta_{ss'}\delta_{s0}(1 - T(b)), \tag{5}$$

where $T(b)$ is an impact-parameter dependent transmission coefficient that takes into account the probability of projectile-target interactions more complex than those being discussed here. We approximate the transmission coefficient as

$$T(b) = \frac{1}{1 + \exp((b - R)/a))}, \tag{6}$$

where we take the strong-interaction radius to be $R = 1.23(A_P^{1/3} + A_T^{1/3})$ fm and the diffusivity to be $a = 0.50$ fm, with A_P and A_T the projectile and target mass numbers, respectively.

As the only coherent coupling in the time-evolution equation is through the collective interaction V, which couples only collective states having the same statistical index s, we conclude that the density matrix will remain diagonal in the statistical index s at all times,

$$\rho_{ns,n's'}(t) = \delta_{ss'}\rho_{ns,n's}(t). \tag{7}$$

The density matrix thus reduces to a separate density submatrix for each value of the statistical index, with the coupling between these submatrices, through the gain and loss terms, being completely incoherent.

It is convenient to explicitly take into account the time dependence due to the collective excitation energy. To do this, we define a modified density matrix, which will have the same diagonal matrix elements as the original one, as

$$\rho^s_{nn'}(t) = \exp\left[-i(\varepsilon_n - \varepsilon_{n'})t/\hbar\right] \rho_{ns,n's}(t). \tag{8}$$

The time evolution equation then reduces to the form

$$\begin{aligned} \hbar\frac{\partial \rho^s_{nn'}}{\partial t} = -i\sum_m \left(\tilde{V}_{nm}(t)\rho^s_{mn'} - \rho^s_{nm}\tilde{V}_{mn'}(t)\right) \\ -\frac{(\Gamma_{ns} + \Gamma_{n's})}{2}\rho^s_{nn'} + \delta_{nn'}\sum_{r,m}\Gamma_{ns\leftarrow mr}\rho^r_{mm}, \end{aligned} \tag{9}$$

in which the remaining contribution to the coherent evolution is due to $\tilde{V}$, where

$$\tilde{V}_{nn'}(t) = \exp\left[i(\varepsilon_n - \varepsilon_{n'})t/\hbar\right] V_{nn'}(t). \tag{10}$$

The second line of Eq.(9) contains the incoherent contributions of the statistical loss and gain terms, respectively.

Assuming that the collective excited states are harmonic n-phonon giant dipole states, the interaction matrix elements can be written as

$$\tilde{V}_{nn'}(t) = \left(\exp\left[i\varepsilon_d t/\hbar\right]\sqrt{n}\delta_{n',n-1} + \exp\left[-i\varepsilon_d t/\hbar\right]\sqrt{n+1}\delta_{n',n+1}\right) V_{01}(t) \tag{11}$$

where ε_d is the excitation energy of the giant dipole resonance and $V_{01}(t)$ is the semiclassical matrix element coupling the ground state to the giant resonance, which we take to have the simple form

$$V_{01}(t) = V_0\frac{(b_{\min}/b)^2}{1+(\gamma v t/b)^2}, \tag{12}$$

as given in Ref. 8. As is done there, we neglect the spin degeneracies and magnetic multiplicities of the giant resonance states and approximate the projectile-target relative motion as a straight line.

The decay widths in the case of harmonic phonons can be approximated as

$$\Gamma_{ns} = n\Gamma_d, \tag{13}$$

where Γ_d is the spreading width of the giant dipole resonance. We have neglected the contribution to the width of the hot statistical background of states since, at the low temperatures

involved here, the decay widths of the hot Brink-Axel resonances are very similar to those of the cold ones.

According to the convention we have adopted for labeling states, the statistical index denotes the number of collective phonons that have decayed to the incoherent statistical background. The decay of the n-phonon s-background state thus transfers its occupation probability to the $(n-1)$-phonon $(s+1)$-background state. The form of the gain terms reflects this fact,

$$\Gamma_{ns\leftarrow mr} = \delta_{s,r+1}\delta_{n,m-1}\Gamma_{mr} = \delta_{s,r+1}\delta_{n,m-1}m\Gamma_d. \tag{14}$$

We solve the differential equations numerically. A typical solution is shown in Figs. 4 and 5, where we display the time dependence of the occupation probabilities (diagonal elements of the density matrix) of the zero-, one- and two-phonon states, for the system ^{208}Pb + ^{208}Pb at an incident energy of 200 MeV per nucleon and an impact parameter of b=15 fm. For the centroid and width of the giant dipole resonance, we use values taken from a global systematic, $\varepsilon_d = 43.4\,A^{-0.215}$ MeV and $\Gamma_d = 0.3\,\varepsilon_d$ [17], giving $\varepsilon_d = 13.8$ MeV and $\Gamma_d = 4.1$ MeV, slightly above the experimental values.

In Fig. 4, we see that the ground state occupation probability drops rapidly in the first half of the collision, while the occupation of the collective one-phonon state rises accordingly. The occupation probability of the decayed one-phonon state follows more slowly but, by the midpoint of the collision, at $t = 0$, is about 25% of the value of the occupation of the coherent one-phonon state. We find the tendency of the two-phonon states in Fig. 5 to be similar. The occupation probability of the coherent two-phonon state rises first, with that of the one-coherent, one-decayed phonon state following more slowly but attaining a value of about 50% of that of the collective one at the midpoint of the collision. The one-coherent, one-decayed phonon state is occupied both through the decay of the coherent two-phonon state and through collective excitation of the decayed one-phonon state. The occupation probability of the two-decayed-phonon state grows more slowly than the others, as it is occupied only through the decay of the one-coherent, one-decayed phonon state.

We observe in Figs. 4 and 5 that all states eventually decay to the states containing no collective excitations,

$$\rho^s_{nm}(t \to \infty) \to 0 \qquad n, m \neq 0. \tag{15}$$

We can define asymptotic occupation probabilities for the states with no collective excitations as

$$\rho^s_{00}(t \to \infty) \to P^s_0, \tag{16}$$

where probability conservation requires that

$$\sum_s P^s_0 = 1 - T(b), \tag{17}$$

with $T(b)$ the transmission coefficient of Eq.(6).

Although the states containing collective phonons are asymptotically depopulated, we can still obtain an estimate of the probability that passes through them by calculating the probability that decays out of them. We thus define for these states

$$P^s_n \equiv \Gamma_{ns} \int_{-\infty}^{\infty} dt\, \rho^s_{nn}(t) \qquad n \neq 0. \tag{18}$$

We note that this is only an estimate of the probability that has passed through each state, as it takes into account only that part of the probability that decays incoherently. It does not include the fraction of the probability that was transferred coherently (through the action of V) to other states.

Finally, we define a cross section σ^s_n for each state by integrating its probability P^s_n over the implicit dependence on the impact parameter,

$$\sigma^s_n \equiv 2\pi \int_{b_{min}}^{\infty} b\, db\, P^s_n(b). \tag{19}$$

At extremely low energies, the lower limit of the integral over impact parameter, b_{min}, is determined by the classical point of closest approach of the Coulomb interaction. When the energy is sufficiently high to surpass the Coulomb barrier, the transmission coefficient $T(b)$ cuts the integral off at low values of the impact parameter.

III. NUMERICAL CALCULATION OF MULTIPHONON EXCITATION

We have performed calculations of multiple giant dipole resonance excitation within the model for the system ^{208}Pb + ^{208}Pb in the projectile energy range from 100 to 1000 Mev/nucleon. We display in Fig. 6, as a function of the projectile energy, the coherent n-phonon cross sections σ_n^0 (dashed lines) and total n-phonon cross sections σ_0^n (solid lines) obtained from the calculation. The coherent cross sections σ_n^0 describe the direct excitation of the n-phonon states. These are the cross sections that result from a standard calculation of multiple giant resonance excitation amplitudes. The total n-phonon cross sections σ_0^n account for all possible n-phonon excitations, including those in which one or more of the phonons decays incoherently before others are excited. The respective coherent or total cross sections decrease by about an order of magnitude for each additional phonon of excitation. The coherent n-phonon cross sections increase monotonically with energy, as do the total excitation cross sections for low phonon number. For the cases of three phonons, the total n-phonon cross section first decreases with the incident energy, but then turns and increases like the other cross sections.

Except for the 1-phonon case, the total n-phonon cross sections σ_0^n in Fig. 6 are clearly larger than the coherent cross sections σ_n^0. This can be readily understood by noting that, although there is only one way a single phonon can be excited and decay, alternative sequences of excitation and decay are available when more than one phonon is involved. As we have emphasized previously in the case of 2-phonons [12–14], the total cross section σ_0^2 contains both the coherent 2-phonon excitation, 2-phonon decay contribution σ_2^0 and an incoherent contribution due to the excitation (and decay) of a second phonon after the first phonon has decayed into the statistical background. A part of the apparent discrepancy in experimental double giant dipole resonance cross sections can thus be explained by arguing that what is observed is the total 2-phonon cross section σ_0^2 and not just the coherent cross section σ_2^0.

The relative importance of the coherent excitation cross sections, σ_n^0, compared to the

total ones, σ_0^n, can best be seen by looking at their ratio, σ_n^0/σ_0^n, as shown in Fig. 7 as a function of the projectile energy. We observe that the total n-phonon cross sections σ_0^n are greatly enhanced relative to the coherent cross sections σ_n^0 at low energies. As the energy increases, the relative enhancement decreases and tends toward one. This trend can be explained by comparing the time scale of the collision process to that of the decay of a giant resonance into the statistical background. At low bombarding energy, the collision occurs slowly relative to the decay time of the resonance. Subsequent excitations then usually occur after the previous ones have decayed and the cross sections for coherent multiple excitation are small compared to the total ones. As the energy increases, the collision time decreases and the time available for decay of a phonon before the excitation of another also decreases. The relative importance of the incoherent contributions to the n-phonon excitation cross section thus decreases as does the relative enhancement of the total cross section over the coherent one.

In Fig. 8, we show the differential excitation cross section that we obtain for the system ^{208}Pb + ^{208}Pb at 640 MeV/nucleon as a function of the excitation energy. This was obtained by summing Breit-Wigner expressions with the appropriate excitation energy and width for each of the total n-phonon cross sections. We show only the contributions of the first three giant dipole resonances, as the higher order ones are almost invisible even on our theoretical curve. Only the first and second giant dipole resonances have been observed experimentally.

As the GDR excitation mechanism proposed here does not depend on the peculiarities of the excited nucleus, we expect it to be ubiquitous in the periodic table. We can ask, however, how the energy range in which it is important varies with the mass of the projectile being excited. To estimate this, we compare the collision and GDR decay times and calculate the value of the projectile energy for which the two are equal. For the case of ^{208}Pb, the decay and collision times are equal at $E_P/A_p \approx 150$ MeV, where the DGDR enhancement is about 50%.

To obtain a general estimate, we use a global systematic, $\varepsilon_d = 43.4\, A^{-0.215}$ MeV and $\Gamma_d = 0.3\,\varepsilon_d$ [17], to approximate the decay time, $\tau_d = \hbar/\Gamma_d$. We assume a projectile of mass

A_p incident on ^{208}Pb, to estimate the collision time as

$$\tau_c = \frac{b}{\gamma v} \approx \frac{r_0(A_p^{1/3} + 208^{1/3})}{\gamma v}, \qquad r_0 = 1.23 \text{ fm}.$$

Equating the two expressions yields the curve of Fig. 9. From the figure, we conclude that the energy range in which the fluctuation contribution to the DGDR excitation is important grows slightly larger as the projectile mass decreases.

IV. CONCLUSIONS

In summary, we conclude from the semiclassical calculations presented here that the collective-statistical description of multiple giant resonance excitation provides a theoretical basis for at least a part of the energy-dependent enhancement of multiple excitation cross sections observed experimentally. Although we do not claim that the entire enhancement arises in all cases through this mechanism alone, we have shown that it can produce an important part of the enhancement and should be taken into account before seeking other causes for the experimental observations.

ACKNOWLEDGMENTS

B.V.C, M.S.H. and A.F.R.T.P acknowledge the support of FAPESP. L.F.C., B.V.C. and M.S.H. acknowledge support from the CNPq.

REFERENCES

[1] See eg. H. Emling, Prog. Part. Nucl. Phys. **33,** 729 (1994); Ph. Chomaz and N. Frascaria, Phys. Rep. **252**, 275 (1995).

[2] R. Schmidt *et al.*, Phys. Rev. Lett. **70**, 1767 (1993).

[3] T. Aumann *et al.*, Phys. Rev. C **47**, 1728 (1993).

[4] J.L. Ritman *et al.*, Phys. Rev. Lett. **70**, 533 (1993); **70**, 2659(E), (1993).

[5] J.R. Beene, Nucl. Phys. **A569**, 163c (1993).

[6] K. Boretzky *et al.*, Phys. Lett. B **384**, 30 (1996).

[7] Ph. Chomaz *et al.*, Nucl. Phys. **A318**, 41 (1994).

[8] L.F. Canto, A. Romanelli, M.S. Hussein, and A.F.R. de Toledo Piza, Phys. Rev. Lett. **72**, 2147 (1994); C.A. Bertulani, L.F. Canto, M.S. Hussein, and A.F.R. de Toldeo Piza, Phys. Rev. C **53**, 334 (1996).

[9] C. Volpe, F. Catara, Ph. Chomaz, M.V. Andres, and E.G. Lanza, Nucl. Phys. **A589**, 521 (1995).

[10] P.F. Bortignon and C.H. Dasso, Phys. Rev. C **56**, 574 (1997).

[11] C.A. Bertulani, V.Yu. Ponomarev, and V.V. Voronov, Phys. Lett. B **388**, 457 (1996).

[12] B.V. Carlson, L.F. Canto, S. Cruz-Barrios, M.S. Hussein, and A.F.R. de Toledo Piza,"Multiphonon and "hot"-phonon isovector electric-dipole excitations", Los Alamos e-print nucl-th/9808039, submitted for publication.

[13] L.F. Canto, B.V. Carlson, S. Cruz-Barrios, M.S. Hussein, and A.F.R. de Toledo Piza,"Fluctuation contributions to double giant dipole resonance excitation cross sections", to appear in Proceedings of the XX Brazilian Nuclear Physics Workshop, World Scientific, Sept. 1997.

[14] B.V. Carlson, M.S. Hussein, and A.F.R. de Toledo Piza, Phys. Lett. **B431** (1998) 249.

[15] D. Brink, D. Phil. Thesis, Oxford University, Unpublished (1955); P. Axel, Phys. Rev. **126**, 671 (1962).

[16] C.M. Ko, Z.Phys. **A286**, 405 (1978).

[17] G.Reffo, private communication.

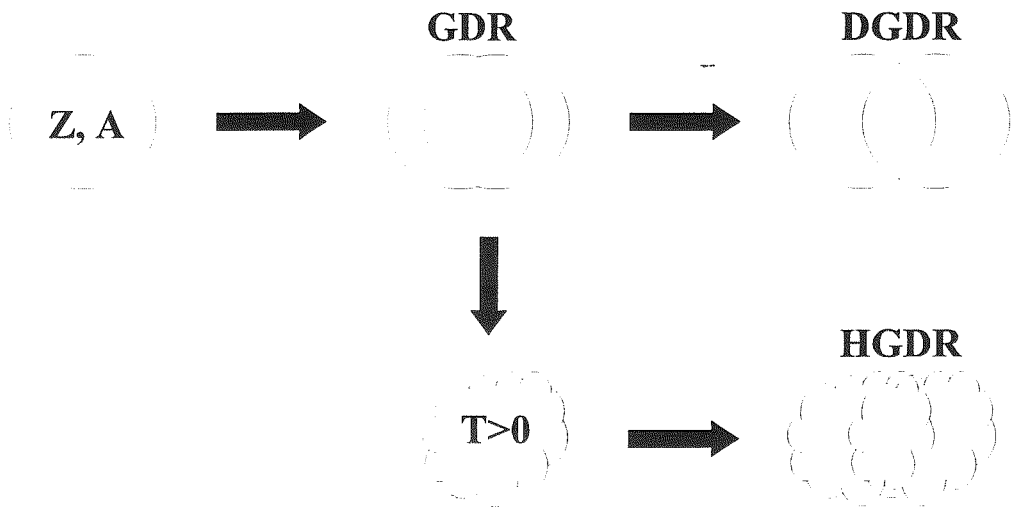

FIG. 1. Cartoon depiction of the conventional double giant dipole resonance excitation (DGDR) and the alternative 'hot' giant dipole excitation (HGDR) described here.

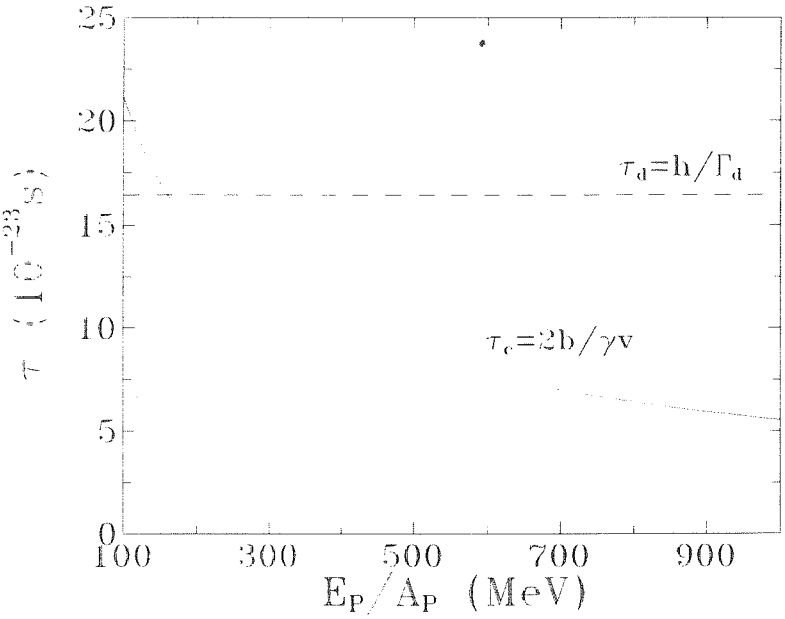

FIG. 2. Collision time τ_c (solid line) and GDR decay time τ_d (dashed line) for the system ^{208}Pb + ^{208}Pb at an impact parameter of 15 fm as a function of the projectile energy per nucleon.

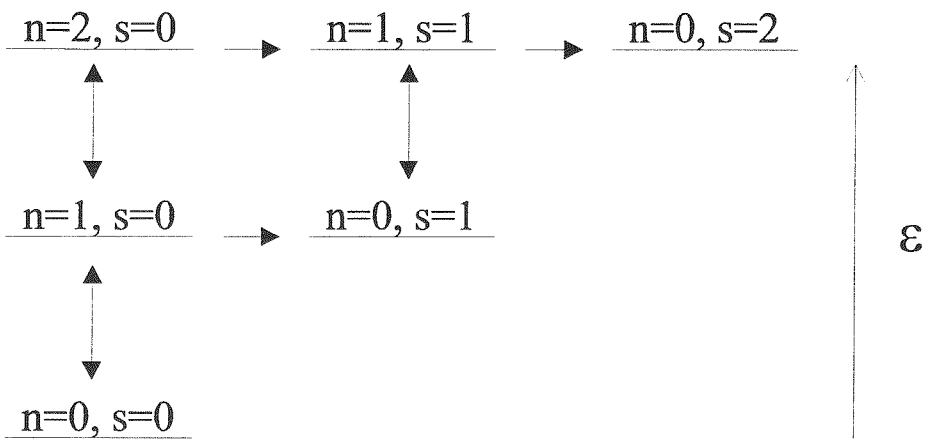

FIG. 3. Schematic representation of the collective/statistical states and their transitions. The vertical arrows represent the two-way coherent excitation/de-excitation of collective phonons. The horizontal arrows represent the one-way statistical decay of the collective phonons. ε denotes the excitation energy.

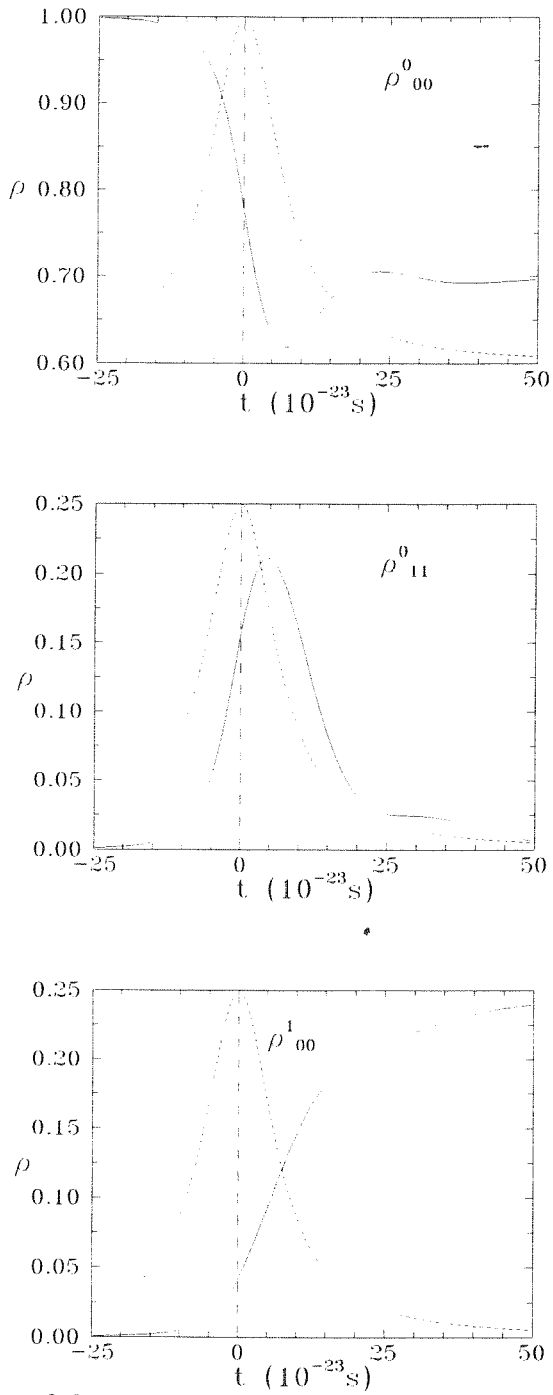

FIG. 4. Time dependence of the occupation probabilities of the ground state and coherent and statistical (decayed) one-phonon states for the system ^{208}Pb + ^{208}Pb at an incident energy of 200 MeV per nucleon and an impact parameter of 15 fm. The dotted line denotes the time dependence of the collective interaction.

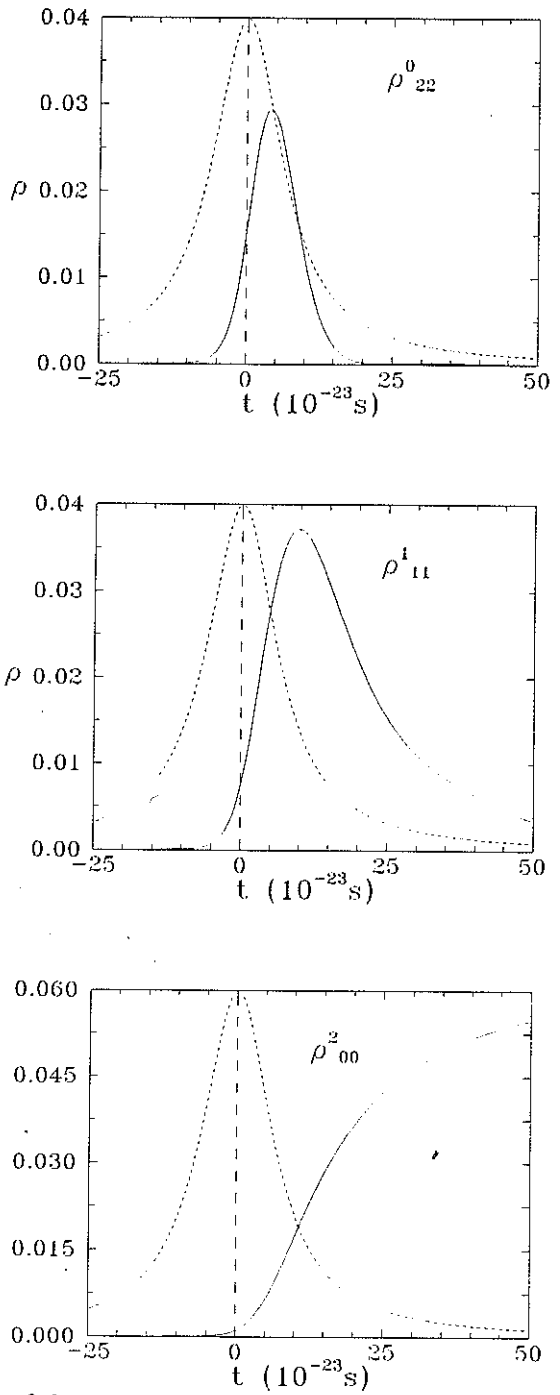

FIG. 5. Time dependence of the occupation probabilities of the two-phonon states (two coherent phonons, one coherent and one decayed phonons and two decayed phonons) for the system ^{208}Pb + ^{208}Pb at an incident energy of 200 MeV per nucleon and an impact parameter of 15 fm. The dotted line denotes the time dependence of the collective interaction.

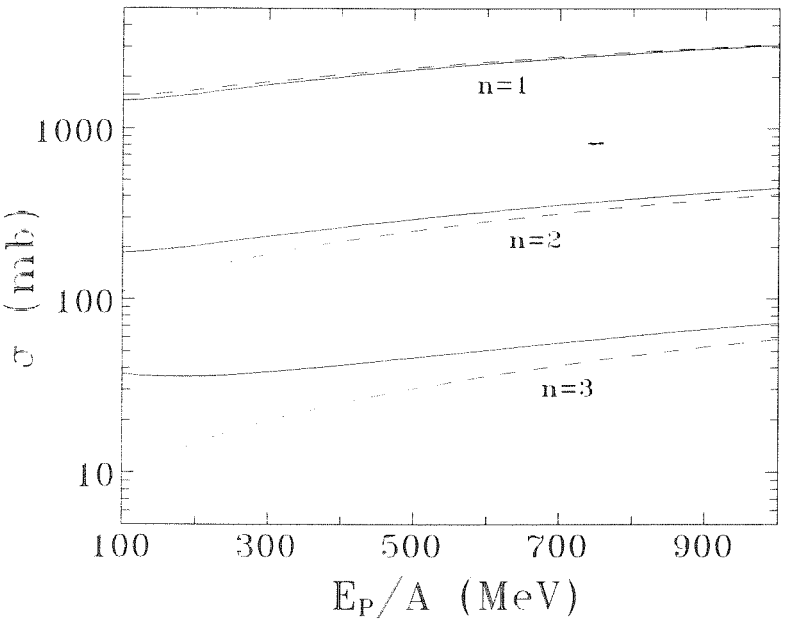

FIG. 6. Total n-phonon excitation cross sections σ_0^n (solid lines) and coherent n-phonon excitation cross sections σ_n^0 (dashed lines) for the system ^{208}Pb + ^{208}Pb as a function of the projectile energy.

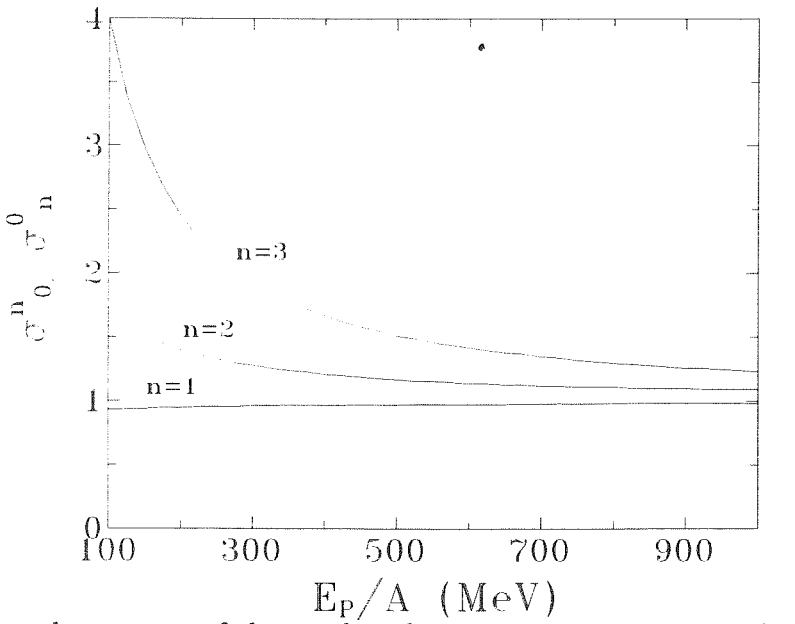

FIG. 7. Relative enhancement of the total n-phonon excitation cross section σ_0^n over the coherent excitation cross section σ_n^0 for the system ^{208}Pb + ^{208}Pb as a function of the projectile energy.

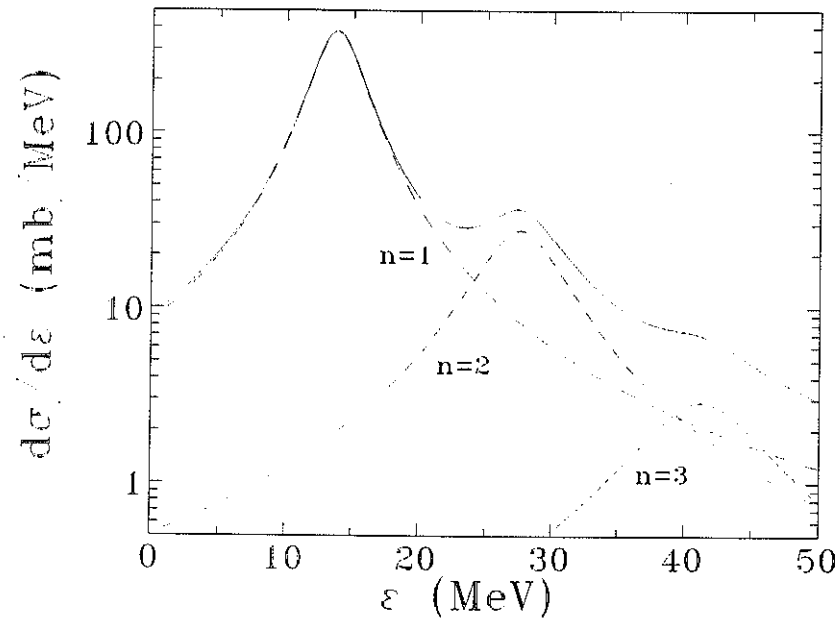

FIG. 8. Theoretical multiple giant resonance differential excitation cross section of ^{208}Pb at a projectile energy of 640 MeV/nucleon.

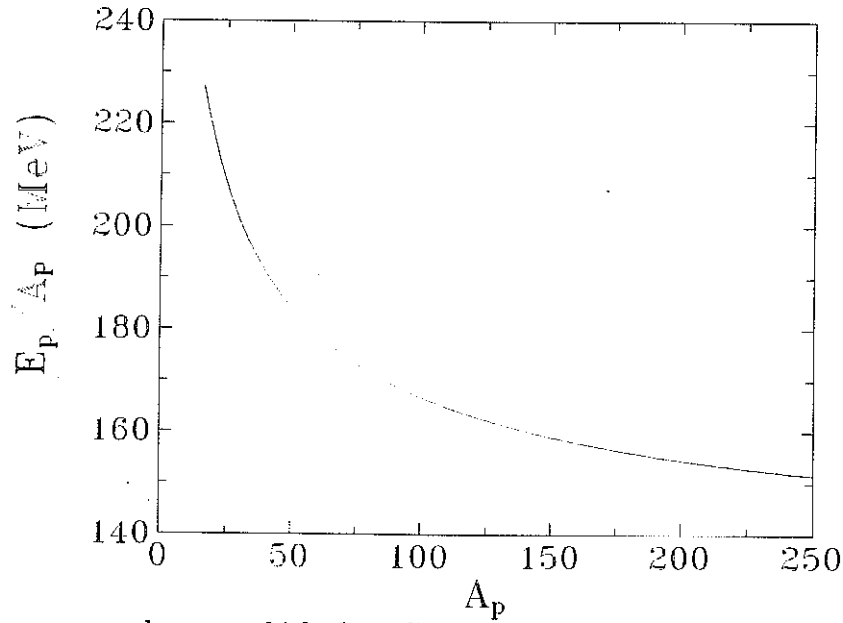

FIG. 9. Energy per nucleon at which the collision time and giant dipole resonance decay time of a projectile in a collision with ^{208}Pb are approximately equal, as a function of the mass number of the projectile.